Fourier-Transform Infrared Studies of CaATPase Partitioning in Phospholipid Mixtures of 1,2-Dipalmitoylphosphatidylcholine-d_{62} with 1-Palmitoyl-2-oleoylphosphatidylethanolamine and 1-Stearoyl-2-oleoylphosphatidylcholine†

M. Jaworsky and R. Mendelsohn*

Department of Chemistry, Olson Laboratories, Newark College of Arts and Sciences, Rutgers University, Newark, New Jersey 07102

Received December 4, 1984

ABSTRACT: CaATPase from rabbit sarcoplasmic reticulum has been reconstituted into binary lipid mixtures of 1-palmitoyl-2-oleoylphosphatidylethanolamine (POPE)/1,2-dipalmitoylphosphatidylcholine-d_{62} (DPPC-d_{62}) and 1-stearoyl-2-oleoylphosphatidylcholine (SOPC)/DPPC-d_{62}. Fourier-transform infrared (FT-IR) spectroscopy has been used to monitor temperature-induced structural alterations in the individual lipid components in the presence and absence of protein. A simple two-state model is used to construct a phase diagram that is in good agreement with one constructed from differential scanning calorimetry data, for the POPE/DPPC-d_{62} (protein-free) system. Although these two lipids are miscible over at least most of the composition range, substantial deviations from ideal behavior are observed. An estimate of the nonideality of mixing in both the gel and liquid-crystalline phases is obtained from regular solution theory. The phase diagram for SOPC/DPPC-d_{62} shows gel-phase immiscibility. FT-IR studies of ternary (POPE/DPPC-d_{62}/CaATPase) complexes indicate that both lipid components are disordered by protein at all temperatures studied. In addition, their melting events are broadened and shifted to lower temperatures compared with the appropriate binary lipid mixture. Semiquantitative estimates for the fraction of each lipid melted are obtained from the model. The effect of protein on SOPC/DPPC-d_{62} mixtures depends on the total lipid to protein ratio. At low protein levels, SOPC is preferentially selected by CaATPase, so that bulk lipid is enriched in DPPC-d_{62}. At high levels of protein, both lipid components are selected. The applicability of vibrational spectroscopy for determination of the partitioning preferences of membrane proteins into regions of particular chemical structure or physical order in a complex lipid environment is demonstrated.

The well-documented dependence of membrane-bound enzyme activity in reconstituted systems upon the chemical structure or physical state of the phospholipid environment [for reviews, see Gennis & Jonas (1977) and Parsegian (1982)] is likely to have functional consequences in native membranes. To understand the molecular basis of this dependence, many physical studies of protein–lipid interaction have been directed toward determination of changes in the conformation or dynamics of either the lipid or protein component upon their mutual association in vitro.

The majority of such studies have used a single lipid species (not infrequently, a disaturated phosphatidylcholine). Yet such an approach, although essential as a starting point for understanding protein-induced perturbations of lipid organization and lipid-induced alterations in protein structure, dynamics, and function, cannot portray a completely realistic picture of the in vivo possibilities. The complexity of lipid organization possible in native membranes can only be approached through studies of lipid mixtures. In such systems, the occurrence of different phospholipid classes and chain lengths presents possibilities for lipid-phase organization not available for a single lipid species. The simplest model systems that can mimic some expected native membrane properties while remaining amenable to physical studies are binary mixtures of phospholipids. The thermodynamics of such systems has been summarized elegantly (Lee, 1977a,b).

This study reports a method that permits the determination of melting behavior and structural alterations for each lipid component in a binary lipid mixture both in the presence and in the absence of a native membrane protein. The primary technique to be used for study of structural changes is Fourier-transform infrared (FT-IR)[1] spectroscopy. In reconstituted and native systems, the method has been used to monitor changes in both lipid configuration and protein secondary and tertiary structure without the use of possibly perturbing probe molecules (Mendelsohn et al., 1981; Dluhy et al., 1983; Cortijo et al., 1982; Rothschild et al., 1980, 1981). In this work, a membrane-bound enzyme is reconstituted into binary lipid mixtures where one of the lipids selected has its acyl chains perdeuterated. This approach (Mendelsohn & Maisano, 1978) permits the (structurally sensitive) C–D stretching vibrations of the deuterated species to be monitored simultaneously with the (structurally sensitive) C–H vibrations of the remaining nondeuterated species. Thus, order changes and melting phenomena for each lipid component may be separately elucidated (Dluhy et al., 1983; Mendelsohn et al., 1984a,b). In addition, a simple two-state model (Dluhy et al., 1983) allows phase diagrams for the binary lipid mixture to

† This work was supported by grants to R.M. from the National Institutes of Health (GM 29864) and from the Busch Memorial Fund of Rutgers University.

[1] Abbreviations: POPE, 1-palmitoyl-2-oleoylphosphatidylethanolamine; DPPC, 1,2-dipalmitoylphosphatidylcholine; DPPC-d_{62}, acyl chain perdeuterated DPPC; SOPC, 1-stearoyl-2-oleoylphosphatidylcholine; FT-IR, Fourier-transform infrared; ESR, electron spin resonance; NMR, nuclear magnetic resonance; SR, sarcoplasmic reticulum; DPPE, 1,2-dipalmitoylphosphatidylethanolamine; DOPC, 1,2-dioleoylphosphatidylcholine.

0006-2960/85/0424-3422$01.50/0

be constructed. Differential scanning calorimetry experiments (also used to construct phase diagrams) are used to verify the validity of the FT-IR approach in protein-free systems. The advantage of the FT-IR approach arises in ternary systems, where DSC data are difficult (or impossible) to acquire.

The protein selected for the current work is Ca^{2+}-ATPase (ATP phosphohydrolase, EC 3.6.1.3) isolated from rabbit skeletal muscle. This choice is appealing as techniques have been developed in many laboratories (Warren et al., 1974a,b; Hidalgo et al., 1976; McIntyre et al., 1982) for exchange of endogenous with exogenous lipid, with retention of enzymatic activity. Two lipid mixtures that mimic to some extent the lipid composition of native sarcoplasmic reticulum are used in the current experiments, namely, 1-palmitoyl-2-oleoylphosphatidylethanolamine (POPE) in binary combination with acyl chain perdeuterated dipalmitoylphosphatidylcholine (DPPC-d_{62}) as well as 1-stearoyl-2-oleoylphosphatidylcholine (SOPC)/DPPC-d_{62} mixtures. The phase behavior of the former mixture has apparently not been reported, while the latter mixture (with unlabeled DPPC) shows gel-state immiscibility at DPPC concentrations of less than 50 mol % (Davis et al., 1980).

Materials and Methods

Sarcoplasmic Reticulum Isolation and Reconstitution. Crude sarcoplasmic reticulum was isolated from the back and leg muscles of albino rabbits as described (MacLennan, 1970). Further purification and exchange of endogenous lipids was accomplished with a deoxycholate-mediated exchange protocol first described by Warren et al. (1974b) and later modified (Hidalgo et al., 1976). The following weight ratios (protein/deoxycholate/phospholipid) were used for the indicated samples: POPE/DPPC-d_{62}/CaATPase (lipid mole ratio 58/42, total lipid/protein 11:1), 1/0.75/2; POPE/DPPC-d_{62}/CaATPase (lipid mole ratio 65/35, total lipid/protein 56:1) 2/1/6; SOPC/DPPC-d_{62}/CaATPase (lipid mole ratio 67:33, total lipid/protein 30:1), 1/0.75/2; SOPC/DPPC-d_{62}/CaATPase (lipid mole ratio 50:50, total lipid/protein 61:1), 1/1/2. Samples were purified by layering them on a discontinuous sucrose density gradient (15%/50%) and centrifuging them overnight at 150000*g*.

Vesicles were assayed for lipid chain length distribution by gas chromatography of their methylated acyl chains. The lipids were transesterified with 5% (w/w) HCl in MeOH and extracted with diethyl ether. The methyl esters were analyzed on a Hewlett-Packard 5750 gas chromatograph equipped with a column of 5% DEGS Chromosorb W, 80–100 mesh, by using a temperature program of 80–260 °C.

ATPase activity measurements were accomplished with a coupled enzyme assay system (Warren et al., 1974a,b). Lipid concentrations were determined as lipid phosphorus (Chen et al., 1956) following extraction of the lipids with organic solvents. Protein concentration was determined by the method of Lowry et al. (1951). The level of purity of protein in the reconstituted complexes was evaluated with SDS gel electrophoresis (Weber & Osborn, 1969). The 8% cylindrical gels were stained with Coomasie blue and scanned with a densitometer.

Binary Lipid Complexes. The appropriate mole ratios of the lipids were dissolved in $CHCl_3$, dried in vacuo under a stream of N_2 gas, evacuated in a desiccator (<1 Torr) for 3–10 h to remove any traces of residual solvent, and rehydrated at temperatures above the completion of the melting for the particular sample.

FT-IR. The samples were examined in a Harrick cell (25 μm path length) equipped with CaF_2 windows. Spectra were recorded on a Mattson Instruments, Sirius 100 spectrometer equipped with a liquid nitrogen cooled mercury–cadmium–telluride detector. Routinely, 100 interferograms were collected, coadded, apodized with a triangular function, and Fourier transformed to give a resolution of 4 cm^{-1} with data encoded every 2 cm^{-1}. Temperature was controlled with a Haake FK circulating bath and monitored with a Bailey BAT-12 digital thermometer, with a thermocouple sensor placed close to the IR windows in the cell. Frequencies were measured with a center of gravity routine (Cameron et al., 1982), using all points with intensities at 80% or greater of the peak maximum. The precision available routinely was about 0.05 cm^{-1}. Half-widths were determined by interpolation for frequencies at half the peak height. Peak heights were measured by fitting a parabola to the top three data points followed by finding the maximum in the parabola. The spectrum of water (matched for temperture and path length) was subtracted from all data sets. Residual sloping base lines were removed with a linear base-line leveling routine supplied with the instrument software.

Differential Scanning Calorimetry. Calorimetry experiments were performed in a Micro-cal MC1 unit. Sample volumes of 0.70 mL containing about 5 mg of suspension were injected into the sample cell, with the same volume of water or buffer used in the reference cell. Samples were heated at about 24 deg/h following 1–2-h equilibration time in the instrument. Duplicate runs of the same sample gave onset and completion temperatures reproducible to 0.2 °C. Independent samples gave data reproducible to 0.4 °C. Heat capacities were calibrated with a standard electronic pulse, and enthalpies were determined either by cutting and weighing of the peaks or by collection of the data with an A-D converter from Interactive structures, Inc., Bala Cynwyd, PA, and an Apple II+ computer. Duplicate enthalpies are reproducible to about 5–7%.

Materials. Lipids (SOPC, DPPC-d_{62}, and POPE) were purchased from Avanti Polar Lipids (Birmingham, AL), evaluated for purity by thin-layer chromatography, and assayed for chain-length distribution by gas chromatography of their acyl chain methyl esters. Solvents were of the highest purity commercially available. Doubly distilled water was used for all buffers.

Table I: Fatty Acid Compositions for Some Preparations Used in This Study

	sample (lipid/protein mole ratio)		
fatty acid[a]	purified SR (30:1)	SOPC/DPPC-d_{62}/CaATPase (30:1)	POPE/DPPC-d_{62}/CaATPase (56:I)
12:0	0.9		
14:0	0.9	1.9	3.8
16:0[b]	30.4	18.4	32.8
16:0-d_{31}[c]		10.6	29.3
18:0	8.2	26.8	3.4
18:1	22.6	32.2	22.9
18:2	34.7	10.3	7.9
18:3	2.4		

[a] Chain length:number of C=C bonds. [b] Measured as the proteated chain. [c] Measured as the deuterated chain.

Results

Biochemical Characterization of Complexes. The fatty acid composition of the lipid acyl chains for purified SR and for the reconstituted ternary systems studied in this work is shown in Table I. Data for the purified SR are in good agreement with those of Hidalgo et al. (1976) with the exception of the minor components. Data for the ternary reconstituted systems

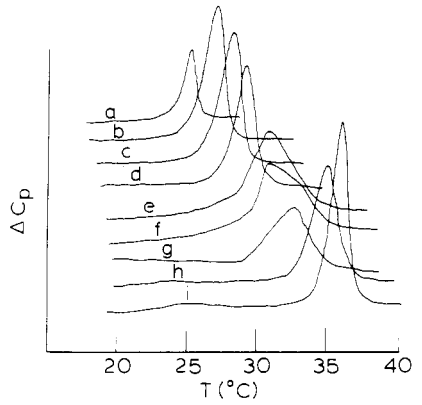

FIGURE 1: DSC traces for POPE, DPPC-d_{62}, and POPE/DPPC-d_{62} binary mixtures as follows: (a) 100:0; (b) 80:20; (c) 67:33; (d) 50:50; (e) 33:67; (f) 20:80; (g) 10:90; (h) 5:95; (i) 0:100. The excess heat capacities plotted on the vertical scale are not comparable from sample to sample.

indicate that high levels of incorporation of the desired phospholipid species have been achieved.

ATPase activities at 37 °C ranged from 2 to 6 IU as monitored with the coupled enzyme assay of Warren et al. (1974a). Densitometer traces (not shown) of polyacrylamide gels of protein in the reconstituted complex showed CaATPase (M_r 110–120 kdaltons) to be the dominant (at least 80–90%) protein species. Electron micrographs (negative staining) showed the presence of unilamellar vesicles.

Binary Lipid Mixtures. (A) Differential Scanning Calorimetry. Experimental DSC curves for pure POPE, DPPC-d_{62}, and several binary lipid mixtures are shown in Figure 1. The main gel to liquid crystal transition for POPE has onset, midpoint, and completion temperatures at 22.4, 25.3, and 26.9 °C, respectively. The midpoint temperature is about 5 °C higher than that observed by Eibl & Wooley (1979), who monitored the transition with a fluorescent probe molecule. The transition width at half-height is 1.2 °C. The calorimetric enthalpy, determined from the area under the excess heat capacity vs. temperature curve, is 3.6 kcal/mol. Also noted (not shown) are endothermic events at higher temperatures. The number, temperatures, and magnitudes of these events depend on the thermal history of the sample. The transitions involved probably reflect formation of hexagonal phases, which are quite easy to form in unsaturated PE's (Cullis & de Kruijff, 1978). For pure DPPC-d_{62}, the main transition has onset, midpoint, and completion temperatures of 33.0, 35.7, and 38.2 °C, respectively. Also noted is a pretransition with onset and completion temperatures of 21.6 and 26.4 °C, respectively. The calorimetric enthalpy is 8.0 kcal/mol. The transition temperatures are in accord with results of Klump et al. (1981).

As the mole fraction of DPPC-d_{62} (the higher melting component) is increased in the mixture from 0 to 0.8 (Figure 1), the onset of melting is slightly shifted toward higher temperatures. The phase diagram for the system is determined from the collection of onset and completion temperatures. These have been plotted in Figure 2. The experimental points have been corrected for the finite width of the melting of the pure components as per the procedure of Mabrey & Sturdevant (1976). While this protocol has little theoretical justification, it minimizes the effects of impurities and instrumental response on the measured melting profiles. The phase diagram in Figure 2 is indicative of nonideal mixing of the two components. It is possible that there are regions of solid-phase immiscibility at low DPPC-d_{62} compositions, but uncertainty in determination of accurate onset temperatures for a transition where melting events begin very gradually (see Figure 1)

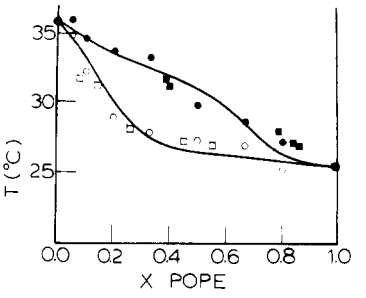

FIGURE 2: Phase diagram for POPE/DPPC-d_{62}. Points from DSC data are (○) onset temperatures and (●) completion temperatures. The procedure of Mabrey & Sturtevant (1976) has been used to correct the data for the finite width of the transitions of the pure components. Points for the solidus (□) and liquidus (■) lines at particular temperatures have been calculated from FT-IR melting curves as discussed in the text. The solid curves are calculated liquidus and solidus lines according to the assumption that the components form a regular solution as discussed in the text. The existence regime for the DPPC-d_{62} pretransition has been omitted.

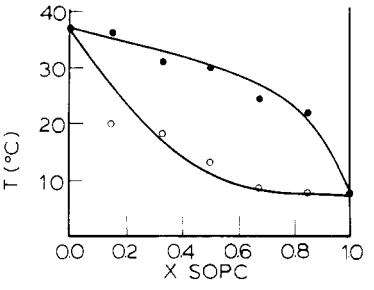

FIGURE 3: Phase diagram for SOPC/DPPC-d_{62}. Points from DSC data are (○) onset temperatures and (●) completion temperatures. Solid lines are intended as a guide for viewing and have *no* theoretical significance.

precludes a definite answer on this point. Also included in Figure 2 is a theoretical simulation of the phase diagram according to the assumption that the components are miscible in both the gel and liquid-crystalline states and form a regular solution. The procedures used for simulation have been discussed by Lee (1977a,b). Regular solutions are characterized by a nonideality parameter related to the heats of mixing (zero for an ideal solution) of the components in the solid and liquid phases. For the theoretical curves shown in Figure 2, the parameters used to achieve the indicated agreement between theory and experiment are ρ_l = 850 cal/mol and ρ_s = 1150 cal/mol, where ρ_l and ρ_s are the liquid- and solid-state nonideality parameters, respectively.

While no "goodness of fit" criterion was employed to achieve the best values of ρ, trial calculations where ρ values differed by more than 50 cal/mol from the selected ones led to substantially worse results, as judged by visual inspection. The magnitude of the nonideality parameters is similar to those used to describe the mixing of different pairs of phosphatidylcholines (Lee, 1977b).

A phase diagram for SOPC/DPPC has been reported by Davis et al. (1980). In this study, the diagram for SOPC/DPPC-d_{62} shows features (Figure 3) quite similar to the earlier work with the proteated species. Regions of gel-phase immiscibility are suggested at mole fractions of DPPC-d_{62} from 0 to about 0.4.

(B) FT-IR Melting Profiles. Typical FT-IR spectral data for the C–H stretching (2800–3000 cm^{-1}) region of a 67:33 POPE/DPPC-d_{62} mixture at several temperatures are shown in Figure 4A. The spectral features arise primarily from the acyl chains of the POPE. Asymmetric and symmetric CH_3 stretching modes appear near 2956 and 2872 cm^{-1}, respec-

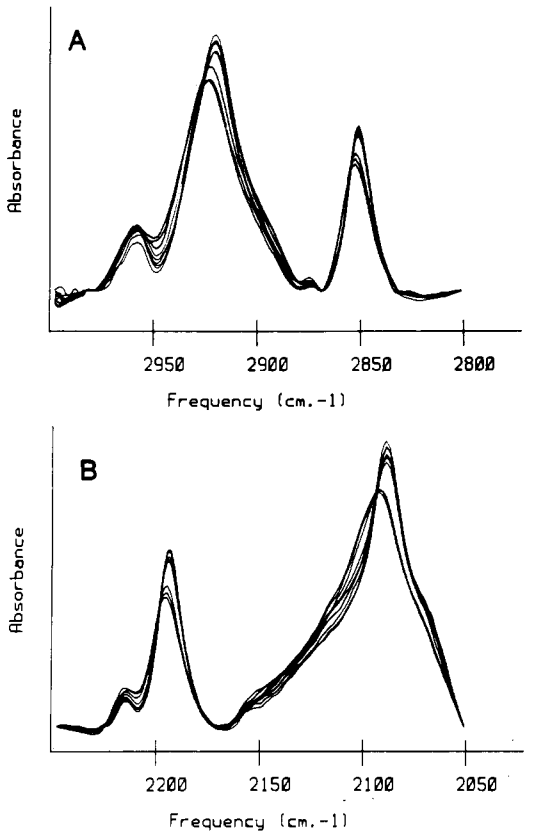

FIGURE 4: (A) FT-IR spectral data for the C–H spectral region (2800–3000 cm^{-1}) for a 67:33 POPE/DPPC-d_{62} mixture at several temperatures. Spectra are plotted at 5 °C intervals. Peak height decreases with increasing temperature. Spectra arise primarily from the POPE component. (B) FT-IR spectral data for the C–D spectral region (2000–2300 cm^{-1}) for a 67:33 POPE/DPPC-d_{62} mixture. See (A) for details. Peaks arise exclusively from the DPPC-d_{62} component.

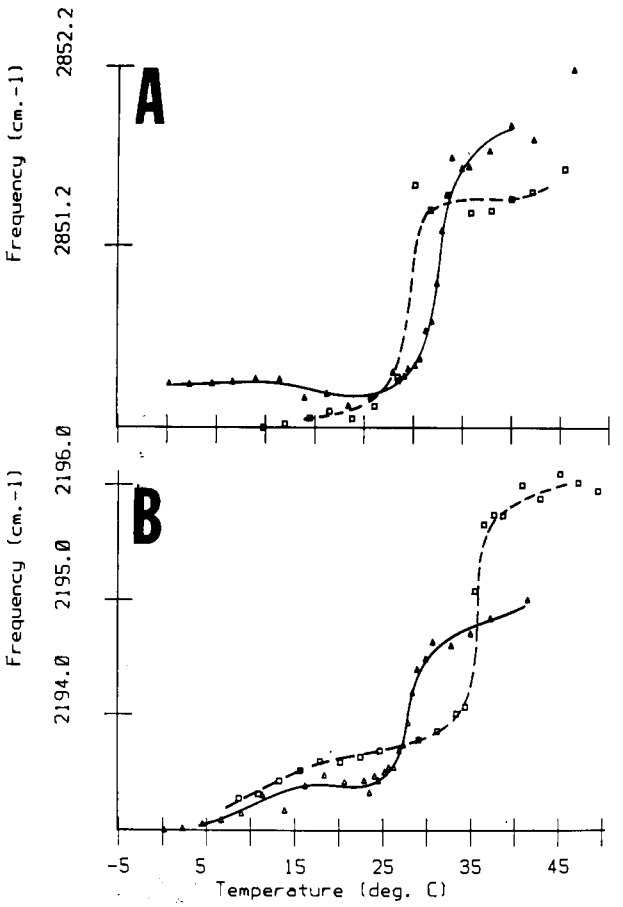

FIGURE 5: (A) Temperature-induced variation in the CH_2 symmetric stretching mode for pure POPE (□) and for the POPE component in a 67:33 POPE/DPPC-d_{62} mixture (▲). (B) Temperature-induced variation in the CD_2 antisymmetric stretching mode for pure DPPC-d_{62} (□) and for the DPPC-d_{62} component in a 67:33 POPE/DPPC-d_{62} mixture (▲).

tively, while the antisymmetric and symmetric CH_2 stretching vibrations are observed at about 2920 and 2850 cm^{-1} (Cameron et al., 1980). In addition, there is a broad Fermi resonance band centered near 2900 cm^{-1} (Snyder et al., 1978).

The 2000–2300-cm^{-1} region of the spectrum contains features arising from the C–D stretching modes of the DPPC-d_{62} component in the binary mixture. Typical data for this spectral region are shown in Figure 4B. The CD_3 groups give rise to bands at 2212 cm^{-1} (asymmetric stretch) and at 2169 cm^{-1} (symmetric stretch). The stronger bands at 2194 and 2089 cm^{-1} arise from antisymmetric and symmetric CD_2 stretching modes, respectively (Cameron et al., 1981).

Alterations in temperature produce changes in the bandwidth and frequency for both the C–H and C–D stretching vibrations, which have been used to characterize the melting of the individual components (Mendelsohn & Maisano, 1978, Dluhy et al., 1983). The frequency of the symmetric CH_2 (for the POPE acyl chains) or antisymmetric CD_2 stretching modes (for the DPPC-d_{62} acyl chains) near 2850 and 2190 cm^{-1}, respectively, are most useful in the present context. The former is not overlapped by protein C–H stretching bands (in ternary complexes consisting of two lipids + protein) while the latter suffers minimal interference from the water-association band near 2100 cm^{-1}. The temperature-induced variation in the CH_2 symmetric stretching mode is plotted for pure POPE and for the POPE component in a 67:33 binary lipid mixture in Figure 5A, while the temperature-induced variation in the CD_2 antisymmetric stretching mode for pure DPPC-d_{62} and for the DPPC-d_{62} component in a 67:33 binary mixture is shown in Figure 5B. The origin of the slight change in these frequencies has been investigated by Snyder et al. (1982) and can be attributed to changes in the interaction constants between C–H stretching coordinates on adjacent methylene groups when the lipid physical state is altered. To convert these melting curves into a quantitative indicator of the fraction of each lipid component melted, a procedure adapted from one outlined earlier (Dluhy et al., 1983) was employed. Briefly, it is assumed that each lipid can exist in one of two physical states characterized by a temperature-dependent Lorentzian distribution for the line shape of the C–H or C–D stretching vibrations. Lorentzian parameters (bandwidths and frequencies) for hypothetical pure gel and liquid-crystalline states of lipid at particular temperatures within the two-phase region are generated from the linear low- and high-temperature regions of the melting curves as shown in the earlier work [Figure 12 of Dluhy et al. (1983)]. The experimentally measured frequency for a particular lipid component is then reproduced according to

$$I(\nu) = (1 - \gamma)\frac{1}{1 + 2(\nu - \nu_g)^2/\alpha_g} + \beta\gamma\frac{1}{1 + 2(\nu - \nu_l)^2/\alpha_l}$$

where $I(\nu)$ = intensity as a function of frequency, γ = fraction of disordered lipid, ν_g = peak frequency for gel-state lipid, α_g = half-width for gel-state Lorentzian, β = relative peak height of the liquid-crystal band, ν_l = peak frequency for the liquid-crystal lipid, and α_l = half-width for the liquid crystalline state Lorentzian. γ is varied until the frequency position at the maximum of the calculated spectrum matches the ex-

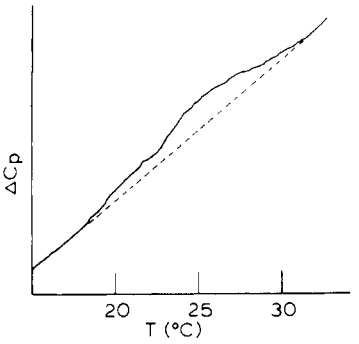

FIGURE 6: DSC trace for a ternary complex of POPE/DPPC-d_{62}/CaATPase: lipid mole ratio 63:35; total lipid/protein 56:1. The dotted line is an interpolation of the linear regions and is the assumed base line.

perimental frequency. Once the values of γ for each lipid component are known, the lever rule and some algebra (Reisman, 1970) allow the utilization of these points for phase-diagram construction.

The points so calculated from the FT-IR melting curves are included in the phase diagram of Figure 2. The reasonable agreement between the DSC data and the FT-IR-constructed points on the phase diagram demonstrates the validity of the FT-IR approach. The advantage of infrared spectroscopy arises in studies of ternary systems. As protein is added to lipid mixtures, the calorimetric transitions broaden and gradually merge with the base lines [e.g., van Zoelen et al. (1978)] so that interpretation is difficult (it being based on the absence of signal). In the FT-IR experiment, although the melting profiles broaden in the presence of protein, signal is observed at all times and at all protein levels. In addition, the melting of each component may be followed if both proteated and deuterated lipid components are used. The application of this method is shown below.

Ternary Systems. (A) Differential Scanning Calorimetry. A DSC trace for a ternary complex of POPE/DPPC-d_{62}/CaATPase (mole ratio POPE/DPPC-d_{62} 65:35, total lipid/protein 56:1) is shown in Figure 6. The cooperativity of the transition is reduced by protein (compared with the binary lipid mixture shown in Figure 1), and the onset of melting is lowered from 24 to 18 °C. It is also evident from Figure 6 that the heat capacity in single-phase regions is substantial, as judged by the slope of the trace below the onset and above the completion temperature for the transition. As the level of protein is increased in the complex, a further broadening of the transition and merging of the DSC curve with the base line occurs, so that at a lipid/protein ratio of 11:1 no cooperative melting event is noted. For the SOPC/DPPC-d_{62}/CaATPase complex, no reproducible cooperative transitions have been observed, even with the rather sensitive Micro-cal MC1 unit available.

(B) FT-IR Data for POPE/DPPC-d_{62}/CaATPase. A plot of frequency vs. temperature for the symmetric CH_2 stretching vibration at 2850 cm^{-1} in the ternary complex (total lipid/protein 56:1, POPE/DPPC-d_{62} 65:35) is shown in Figure 7A along with similar data for the binary lipid mixture of the same composition. Data for the CD_2 symmetric stretching vibrations for the same systems are plotted in Figure 7B. The effect of CaATPase on each component is to reduce the onset and midpoint temperatures of the melting and to broaden the melting range. In addition, each lipid component shows a substantially higher acyl chain frequency (at all temperatures) in the ternary complex compared with the binary mixture, indicative of protein-induced disorder in both gel and liquid-crystal lipid phases. To place these results on a more quantitative basis, the fraction of each lipid melted, determined according to the protocol outlined above, is plotted in Figure 8, for both the binary lipid mixture and the ternary system. It is evident from Figure 8 that both lipids are substantially disordered by CaATPase, so that the onset of melting is about

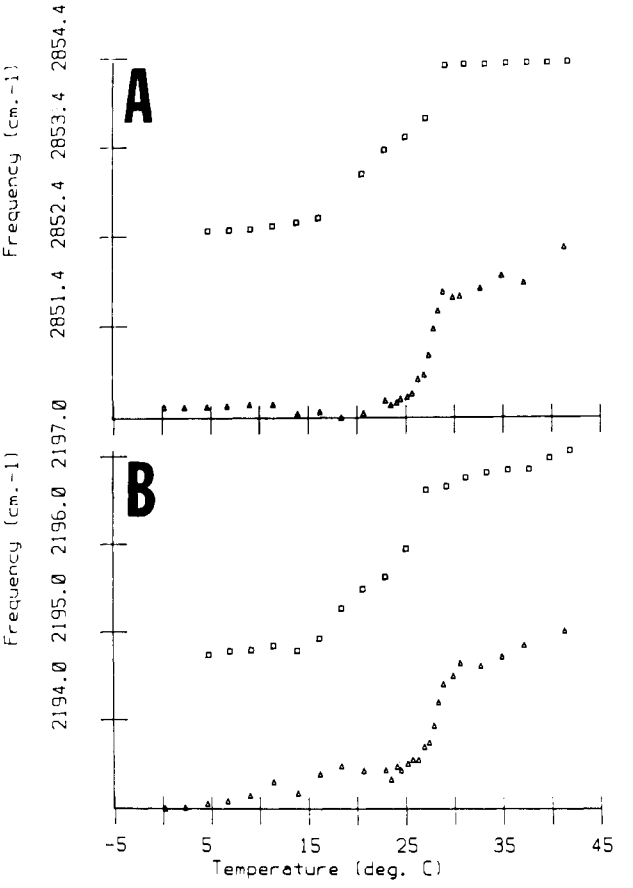

FIGURE 7: (A) Temperature-induced variation for the CH_2 symmetric stretching mode in the ternary complex POPE/DPPC-d_{62}/CaATPase (lipid mole ratio 65:35, total lipid/protein 56:1) (□), as well as for the binary lipid mixture (67:33) (▲) in the absence of protein. (B) Temperature-induced variation for the CD_2 asymmetric stretching mode in the ternary complex POPE/DPPC-d_{62}/CaATPase (□), as well as in the binary lipid mixture (POPE/DPPC-d_{62} 67:33) in the absence of protein (▲).

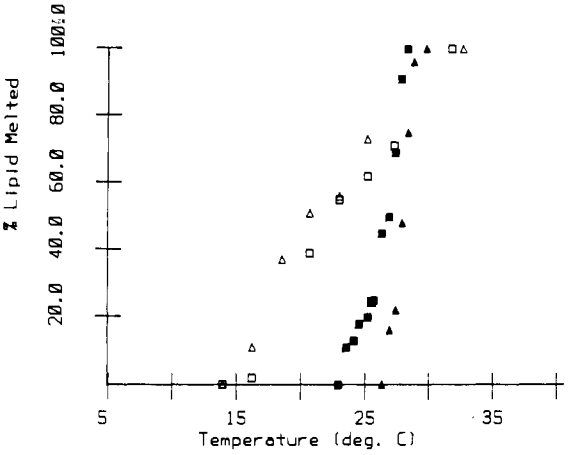

FIGURE 8: Fraction of each lipid component melted calculated as described in the text for (i) the DPPC-d_{62} component in the 67:33 (POPE/DPPC-d_{62}) binary mixture (▲), (ii) the DPPC-d_{62} component in the ternary complex POPE/DPPC-d_{62}/CaATPase (lipid mole ratio 65:35, total lipid/protein 56:1) (△), (iii) the POPE component in the binary mixture described above (■), and (iv) the POPE component in the ternary complex described above (□).

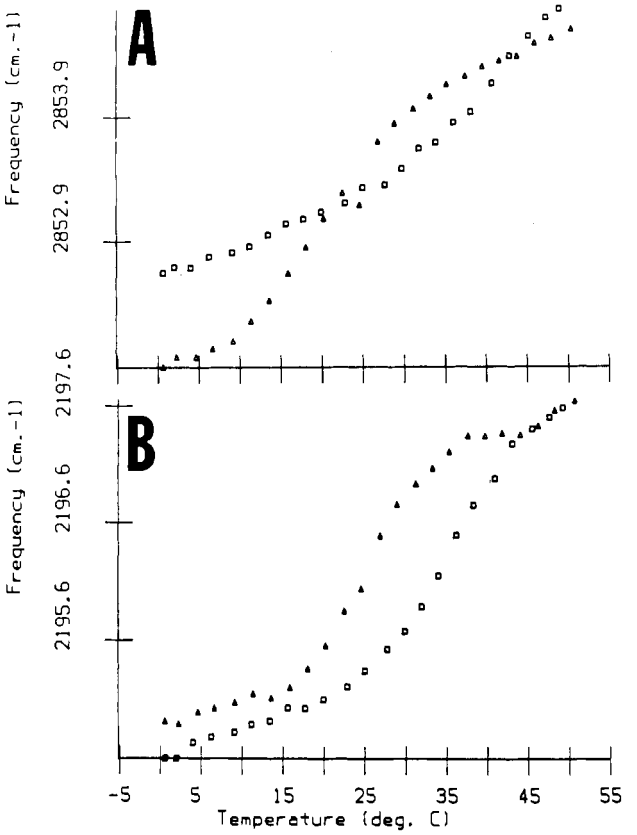

FIGURE 9: (A) Temperature-induced variation in the CH_2 stretching frequency of the SOPC component in an SOPC/DPPC-d_{62} binary lipid mixture (▲) and in the ternary complex SOPC/DPPC-d_{62}/CaATPase (lipid mole ratio 50 50, total lipid/protein 60 1) (□). (B) Temperature-induced variation in the CD_2 asymmetric stretching frequency of the DPPC-d_{62} component in the binary lipid mixture (▲) and ternary complex (□) described above.

7 deg lower for the POPE component and about 13 deg lower for the DPPC-d_{62} component in the ternary complex. The completion temperatures are much less altered. The protein-induced disordering and reduction of T_m of each lipid component are more pronounced at higher protein levels. Melting curves (not shown) were generated for the POPE and DPPC-d_{62} components of a ternary system (POPE/DPPC-d_{62} mole ratio 58:42, total lipid/protein 11:1). The melting processes are rendered even less cooperative and shifted to lower temperatures compared with the complexes containing less protein.

(C) FT-IR Data for SOPC/DPPC-d_{62}/CaATPase Complexes. FT-IR data for each lipid component as well as for the appropriate control systems have been obtained for a ternary complex (SOPC/DPPC-d_{62} 67:33, total lipid/protein 30:1; data not shown). The effect of protein is similar to that observed for the POPE/DPPC-d_{62} system. Each lipid component has its melting event broadened or completely abolished and (if broadened) shifted to lower temperatures. In addition, the observation of protein-induced disorder is evident for both lipid components at all temperatures, as shown by increased CH_2 or CD_2 frequencies.

Substantially different behavior is noted for a final ternary complex (SOPC/DPPC-d_{62} 50:50, total lipid/protein 61:1). The FT-IR data for each lipid component as well as for the appropriate control system are shown in panels A (SOPC) and B (DPPC-d_{62} component) of Figure 9. In this sample, the effect of protein is to completely abolish the SOPC melting (Figure 9A), while, in contrast, to shift to higher temperatures and slightly sharpen the transition of the DPPC-d_{62} component (Figure 9B). In addition, a protein-induced ordering of the deuterated component is noted. Since the effect of protein on DPPC alone is to reduce T_m with little change in order (Mendelsohn et al., 1984), the implication of the results in Figure 9 is that DPPC-d_{62} is excluded from interaction with protein in this ternary complex. Bulk lipid is enriched in DPPC-d_{62}, leading to domains of this molecule that melt at temperatures substantially higher than those in the control system.

Discussion

The advantages of FT-IR spectroscopy for studies of lipid–protein interaction are amply demonstrated in this work. The good agreement shown in Figure 2 for points on the phase diagram constructed from DSC compared with FT-IR experimental data justify both the model used to reduce the latter and the assumption that changes in the FT-IR parameters directly reflect changes in lipid order and/or dynamics. The advantages of FT-IR are 2-fold. In situations where DSC data are impossible to acquire, due to either a noncooperative melting process (in some ternary complexes used in the current work, for example) or low inherent enthalpy changes, FT-IR data probe melting events in the system, as the observation of signal does not depend on either the cooperativity or energetics of the melting process. In addition, each component in a binary lipid mixture may be separately monitored.

Contradictory evidence concerning the effect of membrane protein on lipid order/dynamics appears in the literature. Experiments with reconstituted systems involving ESR or ^{31}P NMR spectroscopic (Nakamura & Ohnisihi, 1975; Yeagle, 1982) measurements of lipid properties were interpreted in terms of two distinct lipid populations—one with motional characteristics only slightly altered from pure lipid and the other with characteristics of an immobilized component. In contrast, more recent studies of sarcoplasmic reticulum involving ^{31}P NMR and ^{2}H NMR (Rice et al., 1979; Fleischer et al., 1982; McLaughlin et al., 1981) have concluded that a single homogeneous lipid environment exists, at least on the time scale of the NMR experiments. In prior work from this laboratory (Mendelsohn et al., 1984), it was demonstrated that the effect of CaATPase on either native SR lipids or DOPC in reconstituted systems was to induce a slight average ordering of the acyl chains. In contrast, reconstitution experiments with lipids containing two saturated chains such as DPPC or DPPE (R. Mendelsohn and G. Anderle, unpublished results) revealed a slight progressive reduction of the transition temperature as the level of protein was increased.

Finally, experiments with lipids containing a single unsaturated chain (SOPC or POPE) revealed the most dramatic protein-induced perturbations. The gel–liquid-crystal phase transition is abolished at relatively low protein levels. In addition, substantial disorder is induced at all temperatures (R. Mendelsohn and G. Anderle, unpublished results). Evidently, the level of unsaturation present in the acyl chains determines, at least in part, the lipid response to the insertion of proteins.

The results for the POPE/DPPC-d_{62}/CaATPase are consistent with investigations of a single lipid species. It is evident from Figures 7 and 8 that each component is perturbed by protein. In both the gel and liquid-crystalline phases of the lipid mixture, the FT-IR data indicate that each lipid component is disordered by protein. Evidently, CaATPase does not preferentially select either of these lipids but exerts its influence simply by lowering the temperature at which they both melt. In addition, both DSC and FT-IR data show that cooperativity of the melting is reduced by protein. The result

differs from that reported (Mendelsohn et al., 1984) for the DPPC-d_{62}/DOPC system. In that instance, protein partitioned preferentially into the DOPC component. Thus, the partitioning preferences seem to be related to the (gel-phase) miscibility of the lipid pair. If the lipids are immiscibible (as in the DOPC/DPPC-d_{62} system), the protein tends to select the lower melting component. If the lipids are miscible (as in the current instance), protein insertion does not induce lateral phase separation of the components but simply results in a characteristic disordering of each. An additional factor is revealed in the experiments with ternary systems of SOPC/DPPC-d_{62}/CaATPase (Figure 9). At high levels of protein both lipid components appear to be disordered, as in the POPE/DPPC-d_{62}/CaATPase system. However, as the level of protein is decreased (Figure 9), DPPC-d_{62} appears to be excluded from lipid/protein interaction, so that bulk lipid is enriched in that component. The relative concentration of protein in this instance (with a lipid mixture containing regions of immiscibility) determines its partitioning characteristics. At low protein levels, sufficient amounts of the preferred lipid are present to ensure selective incorporation of that molecule into the lipid–protein interface. At high protein levels, the second component must be incorporated as all of the available preferred lipid class has been utilized.

A limitation of the current approach is the lack of a quantitative model for determination of the fraction of each lipid in contact with protein. London & Feigenson (1981) have addressed this question and developed a technique using fluorescence quenching of spin-labeled phospholipids to measure relative binding constants of protein for two competing lipids. The method is the best available to date, but the use of probe molecules may lead to interpretation problems if the spin-labeled lipids have partitioning characteristics different from their unlabeled counterparts. A protocol has recently been developed (Dluhy et al., submitted for publication) for estimating, through Zimm–Bragg theory applied to the FT-IR melting curves, the fraction of each lipid component in a binary mixture that is in a high-energy or interfacial state. The method depends for input on calorimetric enthalpy measurements. It is useful for binary lipid mixtures but difficult to apply to lipid/protein complexes where enthalpy data are not available. Methods are currently being sought to circumvent this problem. If successful, the amount of lipid in contact with protein as a function of temperature will be accessible from the FT-IR experimental data.

Registry No. ATPase, 9000-83-3; DPPC-d_{62}, 29287-66-9; POPE, 26662-94-2; SOPC, 6753-56-6.

References

Cameron, D. G., Casal, H. L., & Mantsch, H. H. (1980) *Biochemistry 19*, 3665–3672.

Cameron, D. G., Casal, H. L., Mantsch, H. H., Boulanger, Y., & Smith, I. C. P. (1981) *Biophys. J. 35*, 1–16.

Cameron, D. G., Kauppinen, J. K., Moffat, D. J., & Mantsch, H. H. (1982) *Appl. Spectrosc. 36*, 245–249.

Chen, P. S., Toribara, T. Y., & Warner, H. (1956) *Anal. Chem. 28*, 1756–1758.

Cortijo, M., Alonso, A., Gomez-Fernandez, J. C., & Chapman, D. (1982) *J. Mol. Biol. 157*, 597–618.

Cullis, P., & de Kruijff (1978) *Biochim. Biophys. Acta 507*, 207–218.

Davis, P. J., Coolbear, K. P., & Keough, K. M. W. (1980) *Can. J. Biochem. 58*, 851–858.

Dluhy, R. A., Mendelsohn, R., Casal, H. L., & Mantsch, H. H. (1982) *Biochemistry 21*, 1170–1177.

Eibl, H., & Wooley, P. (1979) *Biophys. Chem. 10*, 261–271.

Fleischer, S., Hymel, L., Tamm, L., & Seelig, J. (1982) *Biophys. J. 37*, 51–53.

Gennis, R. B., & Jonas, A. (1977) *Annu. Rev. Biophys. Bioeng. 6*, 195–238.

Hidalgo, C., Ikemoto, N., & Gergely, J. (1976) *J. Biol. Chem. 251*, 4224–4232.

Klump, H. H., Gaber, B. P., Peticolas, W. L., & Yager, P. (1981) *Thermochim. Acta 48*, 361–366.

Lee, A. G. (1977a) *Biochim. Biophys. Acta 472*, 237–281.

Lee, A. G. (1977b) *Biochim. Biophys. Acta 472*, 285–344.

London, E., & Feigenson, G. W. (1981) *Biochemistry 20*, 1939–1948.

Lowry, O. H., Rosebrough, N. J., Farr, A. L., & Randall, R. J. (1951) *J. Biol. Chem. 193*, 265–275.

Mabrey, S., & Sturtevant, J. M. (1976) *Proc. Natl. Acad. Sci. U.S.A. 73*, 3862–3866.

MacLennan, D. H. (1970) *J. Biol. Chem. 245*, 4508–4518.

McIntyre, J. O., Samson, P., Brenner, S. C., Dalton, L., & Fleischer, S. (1982) *Biophys. J. 37*, 53–56.

McLaughlin, A. C., Herbette, L., Blasie, J. K., Wang, C. T., Hymel, L., & Fleischer, S. (1981) *Biochim. Biophys. Acta 643*, 1–16.

Mendelsohn, R., & Maisano, J. (1978) *Biochim. Biophys. Acta 506*, 192–201.

Mendelsohn, R., Dluhy, R. Taraschi, T., Cameron, D., & Mantsch, H. H. (1981) *Biochemistry 20*, 6699–6706.

Mendelsohn, R., Anderle, G., Jaworsky, M., Mantsch, H. H., & Dluhy, R. A. (1984a) *Biochim. Biophys. Acta 775*, 215–224.

Mendelsohn, R., Brauner, J. W., Faines, L., Mantsch, H. H., & Dluhy, R. A. (1984b) *Biochim. Biophys. Acta 774*, 237–246.

Nakamura, M., & Ohnishi, S. (1975) *J. Biochem. (Tokyo) 78*, 1039–1045.

Parsegian, A., Ed. (1982) *Biophysical Discussions; Protein-Lipid Interactions in Membranes*, Rockefeller University Press, New York.

Reisman, A. (1970) *Phase Equilibria*, Academic Press, New York.

Rice, D. M., Meadows, M. D., Scheiman, A. O., Goni, F. M., Gomez-Fernandez, J. C., Moscarello, M. A., Chapman, D., & Oldfield, E. (1979) *Biochemistry 18*, 5893–5903.

Rothschild, K. J., DeGrip, W. J., & Sanches, R. (1980) *Biochim. Biophys. Acta 596*, 338–351.

Rothschild, K. J., Zagaeski, M., & Cantore, W. A. (1981) *Biochem. Biophys. Res. Commun. 103*, 483–489.

Snyder, R. G., Hsu, S. L., & Krimm, S. (1978) *Spectrochim. Acta, Part A 34A*, 395–406.

Snyder, R. G., Strauss, H. L., & Elliger, C. A. (1982) *J. Phys. Chem. 86*, 5145–5150.

van Zoelen, E. J. J., Verkleij, A. J., Zwaal, R. F. A., & van Deenen, L. L. M. (1978) *Eur. J. Biochem. 86*, 539–546.

Warren, G. B., Toon, P. A., Birdsall, N. J. M., Lee, A. G., & Metcalfe, J. C. (1974a) *Biochemistry 13*, 5501–5507.

Warren, G. B., Toon, P. A., Birdsall, N. J. M., Lee, A. G., & Metcalfe, J. C. (1974b) *Proc. Natl. Acad. Sci. U.S.A. 71*, 622–626.

Weber, K., & Osborn, M. (1969) *J. Biol. Chem. 244*, 4406–4412.

Yeagle, P. (1982) *Biophys. J. 37*, 227–236.